Pricing Kernels inferred from Bitcoin Options

Master's Thesis

submitted to

Prof. Dr. Wolfgang Karl Härdle (First Examiner)
Prof. Dr. Brenda López-Cabrera (Second Examiner)

Humboldt-Universität zu Berlin
School of Business and Economics

Ladislaus von Bortkiewicz Chair of Statistics

by

Julian Winkel
562959
DOI

in partial fulfillment of the requirements
for the degree of
Master of Science (Statistics)

Berlin, 19.02.2021

Abstract

Bitcoin Pricing Kernels are inferred using a novel data set from Deribit, one of the largest Bitcoin derivatives exchanges. This enables arbitrage-free pricing of various instruments. State Price Densities are estimated with Rookley's method. The underlying asset process is viewed through the lens of a Stochastic Volatility with Correlated Jumps (SVCJ) framework. Shape invariant pricing kernels are reported. Market inefficiencies are assessed based on the shape of the pricing kernels. A trading strategy that exploits these inefficiencies is evaluated.

List of Tables

List of Figures

Abbreviations

AJD	Affine Jump Diffusion
ARA	Absolute Risk Aversion
ATM	At-the-Money
BRC	Blockchain Research Center
BTC	Bitcoin
CC	Cryptocurrencies
CI	Credible Interval
DAX	Deutscher Aktienindex
FOTM	Far-Out-of-the-Money
GARCH	Generalized Autoregressive Conditional Heteroskedasticity
ITM	In-the-Money
IV	Implied Volatility
PD	Physical Density
PK	Pricing Kernel
PnL	Profit and Loss
SIM	Shape Invariant Models
SV	Stochastic Volatility
SVJ	Stochastic Volatility with Jumps
SVCJ	Stochastic Volatility with correlated Jumps
SPD	State Price Density
USD	US-Dollar

Contents

1 Introduction

Since the inception of Bitcoin as proposed by Nakamoto (2009), the electronic peer to peer cash payment system has come a long way. With the rise of diverse exchanges enabling trading of Cryptocurrencies (CC), the introduction of a corresponding derivatives market professionalized the environment. Among those, Deribit Exchange attracts the vast majority of option trading volume. As of 2021-02-15 Deribit manages about two thirds of the Bitcoin option volume, which translates into 24-hour option trading volume of over 22,000 BTC, more than one billion USD (Coinmarketcap 2021).

As derivatives markets are particularly rich in information, their evolution provides a unique opportunity to assess the Bitcoin market. A classical tool to infer key information from an options market are State Price Densities (SPD). SPDs are that risk-neutral probability density, under which investors price derivatives. Hence they reflect investor's expectations about future prices at a fixed point in time, namely option maturity. As probability densities uniquely define the corresponding probability distribution, SPDs enable us "to derive the whole risk-neutral probability distribution of the underlying asset price at the maturity date of the options" (Huynh, Kervella, and Zheng 2002b, 171). Revelation of this distribution provides the key to pricing exotic or illiquid options, such as Bitcoin options, in an arbitrage-free manner (Aït-Sahalia and Lo 1998).

In conjunction with the Physical Density (PD) of Bitcoin returns, Pricing Kernels (PK) can be inferred. The underlying asset process is viewed through the lens of a Stochastic Volatility with Correlated Jumps (SVCJ) framework. Observing a multitude of PKs over time, a common shape is extracted by collapsing the single PKs into a Shape Invariant Model (SIM). Their relationship is shown by means of parameters which govern horizontal and vertical shifts.

Finally, a trading simulation is conducted. If the investors were perfectly rational, then by no-arbitrage arguments, the SPD should be equal to the PD. Using deviations between the densities in order to identify mispriced events, a portfolio is built and its performance evaluated.

2 Literature Review

Breeden and Litzenberger (1978) derive SPDs using Arrow-Debreu prices and Butterfly Spreads. Their paper was the cornerstone for the now existing vast literature on SPDs, which encompasses a variety of approaches.

A particularly useful approach has been presented in Rookley (1997), who develops a nonparametric estimation method for SPDs. Rookley estimates IV smiles by decomposing the functional relationship between implied volatility and moneyness and time-to-maturity. With such an estimate, it is possible to derive the SPD at every point in a robust way. This nonparametric estimation is advantageous over former approaches because it does not assume a functional form for the SPDs or investor prefrences.

Aït-Sahalia, Wang, and Yared (2001) estimate PKs from S&P500 options data and the according return series in order to assess the efficiency of the options market. Departures from SPD and PD are used to identify inefficient pricing. A trading strategy exploiting the skewness and kurtosis of the densities is proposed and shown to have a high Sharpe Ratio.

Grith, Härdle, and Park (2009) estimate shape invariant PKs. With European DAX option and return data, a series of empirical PKs is estimated from 2003 until 2006. While the risk-neutral density is inferred using Rookley's method, the PD is estimated with a GARCH model. The goal is to find a common shape among the empirical PKs and to define the deviations of the individual curves from the reference curve. The deviations are described using a set of parameters for horizontal and vertical shifts away from the reference curve. Furthermore, the paper aids the understanding of investor's risk aversion as well as it provides a link between risk aversion and PKs.

Whereas GARCH models have been proven to be useful in this context, other methods are available in order to estimate PDs. Some interesting approaches are summarized in the following.

Based on the ideas of Cox, Ingersoll, and Ross (1985) as well as Heston (1993), a closed-form solution for affine jump diffusion (AJD) processes has been presented by Duffie, Pan, and Singleton (2000). Generally, AJD processes describe "a jump-diffusion process for which the drift vector, instantaneous covariance matrix, and jump intensities all have affine dependence on the state vector." (Duffie, Pan, and Singleton (2000) first page, intro).

Chen et al. (2018) investigate different AJD approaches for Bitcoin, among which SJ (Stochastic Jump), SVJ (Stochastic Volatility with Jumps) and SVCJ (Stochastic Volatility with correlated Jumps) can be found. Parameter estimation is performed using a Metropolis-Hastings Monte Carlo model and the SVCJ approach is concluded to be best-suited to describe Bitcoin price changes.

Belaygorod (2005) states how to change from the risk-neutral to the physical measure in the discussed stochastic volatility models.

Matic (2020) analyzes the performance of various hedging models for cryptocurrency options. Good performance is presented for the Black-Scholes and the Heston model, while the results of the Merton model cannot compete. However, there is a substantial default probability due to fat tail events, which is probably attributable to jumps.

Perez (2018a) provides a Shiny App that prices potential cryptocurrency options under an SVCJ process.

3 Data

3.1 Data Structure

PDs are estimated based upon Quandl (2020) End-of-Day BTC/USD Prices from 2019-01-01 until 2020-03-01. The information set is artificially restricted to the observation time, e.g. for any orderbooks traded on 2020-09-01, the price of the same day will be used. All SPDs are calculated in a similar manner. For every observed day, all order book changes are collected from the first second until 11:59:59 pm.

With permission of Deribit, executed trades and orderbook changes have been tracked since the beginning of March 2020 on their exchange. The latter is the foundation for this thesis. The data base is available on the Blockchain Research Center (BRC) of Humboldt-Universität zu Berlin.
The full data set includes all parameters that the Deribit API V2.0 returns at the time of collection under the methods

- public/get_last_trades_by_instrument_and_time
- public/get_order_book

Most importantly the results include

- Timestamps
- Greeks
- Implied Volatility
- Tick Direction
- Order Type
- Volume
- Instrument Price (in BTC)
- Strike
- Spot

Apart from negligble downtime, all order book changes and trades are captured for BTC based instruments. All options are European options. All SPDs are estimated using orderbooks only.

Spot prices of the underlying Deribit-BTC-USD-Index are calculated as a weighted BTC/USD price of eleven major crypto exchanges, namely

- Binance
- Bitfinex
- Bitstamp
- Bittrex
- Coinbase Pro
- Gemini
- Huobi
- Itbit
- Kraken
- LMAX Digital
- OKEx

The following explanation is given by Deribit (2020a): "From the 11 exchanges, we exclude all disconnected, administratively turned off and having detected invalid data. Then, the values from remaining sources are sort, truncated to the 0.5% margin around the median price and averaged with equal weight."

3.2 Preprocessing

Despite market maker's obligation to quote all instruments at most of the time (Deribit 2020c), some may not be quoted or only be quoted at the cost of a large spread. The former may for example occur in the form of an implied volatility being zero at the bid. A large part of this can be explained by FOTM contracts, where the bidding minimum tick size exceeds the target IV. Due to rarer observations for options with a larger time-to-maturity τ, it is restricted to be smaller than one quarter of a year. τ is defined in such a manner that one year until maturity means $\tau = 1$.

Those cases, as well as all duplicates, are excluded from the data set in the preprocessing. Additionally, call options are exclusively used in order to estimate the IV surface in Rookley's method. Put-Call-Parity ensures arbitrage-free Put option prices aswell.

As a contract's value differs according to their strike price K and the spot price S, these variables are collapsed into moneyness M, which is defined as the ratio $\frac{S}{K}$ (sometimes vice versa). The positive effects are manifold: First, it increases comparability between different instruments, as IV surfaces and PKs can be compared despite varying spots and strikes. Second, it reduces the amount of parameters in the nonparametric SPD estimation, thus easing the effects of the curse of dimensionality. Third, it indicates the degree of certainty behind an instrument's payoff: An option that is deep in-the-money (ITM), has a high probability for a payout as the spot is far larger than the strike. In such a case, a price drop until maturity may be unlikely. Conversely, an option's value that is far out-of-the-money (FOTM) primarily draws it's value from time to maturity τ and does not carry any intrinsic value (yet).

Furthermore, deep ITM options will have a Black-Scholes Δ close to one, meaning

that a portfolio holding such an instrument will gain proportionally as a response to an increase in the underlying. However, OTM options are cheaper in absolute terms as their value is entirely extrinsic. An investor whose portfolio mainly consists of OTM options may be regarded as risk affine.

To summarize all preprocessing:

- Duplicates are omitted
- Puts are disregarded for SPD estimation (not for trading)
- Moneyness is restricted to be within the interval $[0.7, 1.3]$
- τ is restricted to be within the interval $[0, 0.25]$
- Bid IV must be larger than zero
- SPD estimation is based on a daily information set

 Preprocessing

4 Descriptive Statistics

More than 41 million order book snapshots have been collected on Deribit from 2020-03-04 until 2020-12-12.

As the start of the data collection in March 2020 coincided with the "Corona Crisis" and it's adverse effects on financial markets, it may be insightful to study it's effects on Bitcoin option markets. Figure 1 depicts clearly how the distress caused by the financial "Corona Shock" (and subsequently large, negative returns) translated into higher risk premia as measured by implied volatility. Despite more than doubling the implied volatility on both sides of the spread, Bitcoin options were not overpriced considering the high realized volatility.

The underlying BTC/USD Index in Figure 2 shows how the sudden price drop in early March 2020 translated into higher volatility and recovered subsequently.

Spreads in Figure 1 are calculated as the average IV at the best bid and ask of all available instruments at the end of each day. While one may argue that the large depicted spread may affect small buyers particularly, the institutional side, meaning option writers, have also suffered under the Corona Shock as payouts of the Deribit insurance fund show. The fund, depicted in Figure 3, grows due to liquidation fees applied to unanswered margin calls. Vice versa the fund shrinks when payouts are conducted to compensate option writer defaults. Due to the severity of defaults around 2020-03-12 and 2020-03-13, Deribit has provided additional deposits, which are depicted in Table 1 (Deribit 2020b).

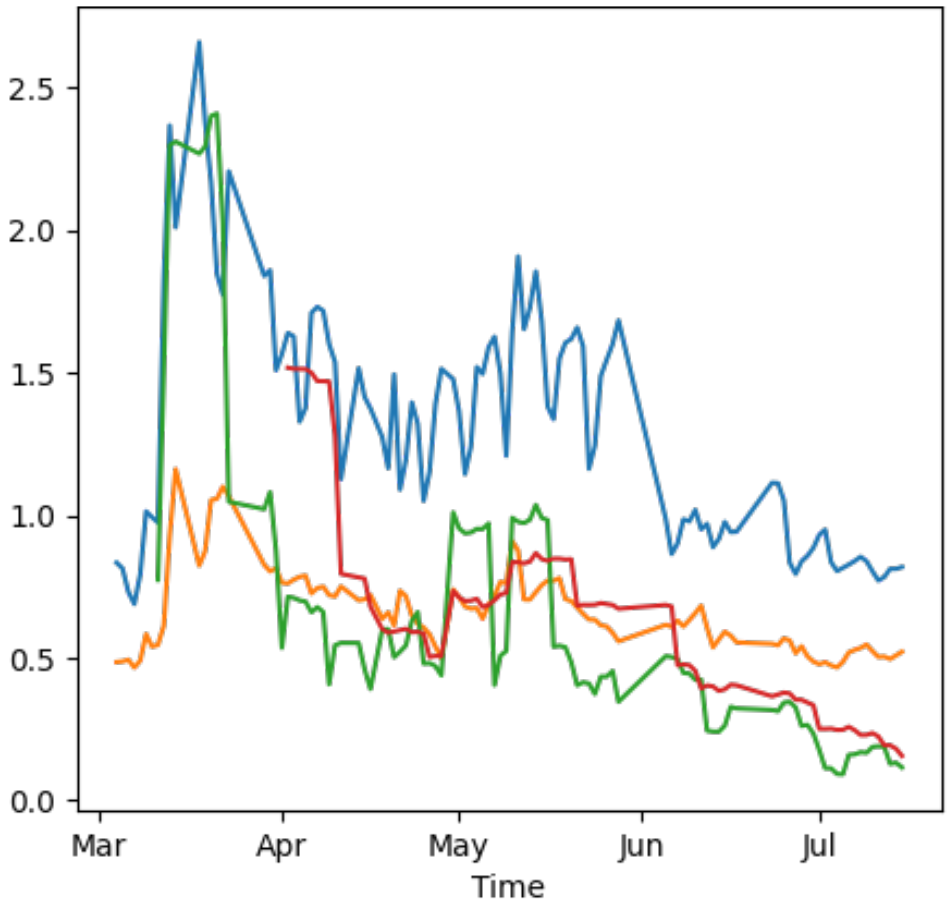

Figure 1: Implied volatility vs. realized volatility. Realized volatility is annualized and regarded in a 7 respectively 21 day window. IV is calculated as the average of observed orderbooks at the bid and ask. Bid IV only considered if larger than zero. Ask IV, Bid IV, 7 Day Volatility, 21 Day Volatility.

Volatility

Figure 2: Average underlying BTC/USD Index per minute. Computed as the average of maximum eleven exchanges as described in the Data Structure section.

Synthetic BTC Index

Date	Deposit
13 March 2020	500
15 March 2020	50
17 March 2020	32
23 March 2020	100
28 April 2020	200

Table 1: Additional Deribit Insurance Fund Deposits in BTC.

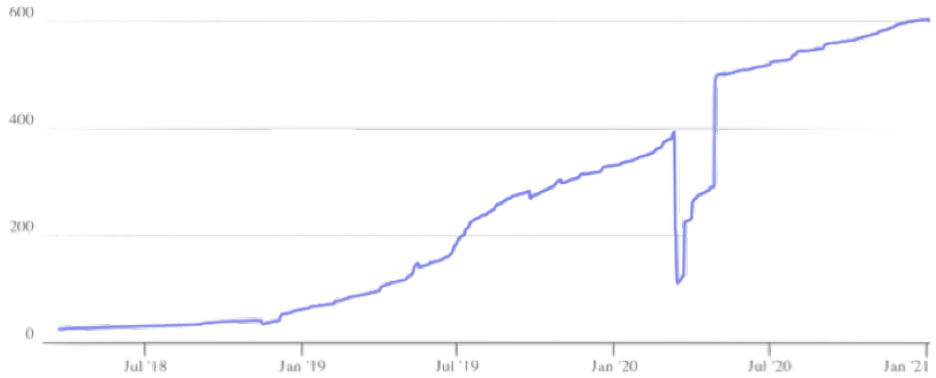

Figure 3: Deribit Insurance Fund payouts show option writer defaults during the Corona Shock. Denoted in Bitcoin.

5 Pricing Kernels

Following Huynh, Kervella, and Zheng (2002a), suppose a risky asset whose price follows a stochastic process $\{S_t\}_{t\in\mathbb{N}}$ and a risk-free interest rate $\{r_t\}_{t\in\mathbb{N}}$ in a complete market.

According to the second Fundamental Theorem of Asset Pricing, a unique martingale-equivalent measure Q exists in the described setting, under which derivatives can be priced in an arbitrage-free manner (Pascucci and Agliardi 2011).

Let C_t be the price at time t of a contingent claim ψ on the risky asset (henceforth: underlying), which has a maturity at T and a time-to-maturity $\tau = T - t$.

The price of any such contingent claim can be expressed as the discounted value of expected future payoffs, weighted with their respective probabilities of occurrence.

$$C_t = e^{-r\tau}\mathrm{E}^Q[\psi(S_T)] = e^{-r_t,\tau}\int_{-\infty}^{\infty}\psi(S_T)f_t^Q(S_T)dS_T \tag{1}$$

Transform the risk-neutral measure Q to the physical measure P.

$$C_t = e^{-r_t,\tau}\int_{-\infty}^{\infty}\psi(S_T)q(S_T)dS_T = e^{-r_t,\tau}\int_{-\infty}^{\infty}\psi(S_T)p(S_T)K(S_T)dS_T \tag{2}$$

where the pricing kernel $K(S_T)$ is defined as $\frac{q(S_T)}{p(S_T)}$

The pricing kernel can be approximated by the ratio of estimates of the risk-neutral density and the physical density. This process is discussed and executed in the following sections. As it is evident from the derivation, the pricing kernel can be used to price arbitrary derivatives.

6 Nonparametric Estimation of State Price Densities

6.1 Derivation

As stated by Breeden and Litzenberger (1978), a SPD can be inferred from the second derivative of the call price function with respect to the strike price.

$$\left.\frac{\delta^2 C_t}{\delta K^2}\right|_{K=S_t} = q(S_T)e^{-r\tau} \tag{3}$$

From the formula it is immediately evident that a variety of call prices C is required in order to calculate the complete SPD q over a range of strike prices K. The present value of a call can be priced in implied volatility, the only real stochastic size of interest. In conjunction with a set of deterministic parameters (time-to-maturity τ, strike K, spot S, interest rate r), the market call price can be calculated. Put prices can be concluded by means of a no-arbitrage approach using Put-Call-Parity.

Implied volatility is estimated as a function of time-to-maturity and moneyness in the following chapter. Using moneyness carries the advantage of reducing the dimensions of spot price S and strike price K into a single size $m = \frac{S}{K}$. The same can be achieved for the remaining parameters as information about the spot price and the interest rate can be collapsed into a Futures price.

6.2 Local Polynomial Estimation

Following Huynh, Kervella, and Zheng (2002b) and Rookley (1997), let the data generating process for implied volatilites be as

$$\sigma = g(M, \tau) + \sigma^*(M, \tau)\varepsilon \tag{4}$$

with a standardized Error ε, Moneyness M, τ and ε independent and $\sigma^*(M, \tau)$ being the conditional variance of σ given $M = m_0$ and $\tau = \tau_0$. Under the assumption that the second derivatives of g exist, g can be approximated using Taylor's Theorem.

Taylor expansion of g in a neighborhood of (m_0, τ_0):

$$\begin{aligned} g(m, \tau) = g(m_0, \tau_0) + \frac{\partial g}{\partial M}(m - m_0) + \frac{1}{2}\frac{\partial^2 g}{\partial M^2}(m - m_0)^2 + \\ \frac{\partial g}{\partial \tau}(\tau - \tau_0) + \frac{1}{2}\frac{\partial^2 g}{\partial \tau^2}(\tau - \tau_0)^2 + \\ \frac{\partial^2 g}{\partial M \partial \tau}(m - m_0)(\tau - \tau_0) \end{aligned} \tag{5}$$

The functional relationship between σ, m and τ can be expressed using a Weighted Least Squares Estimator (WLSE), minimizing the objective function

$$\arg\min_{\beta}(\sigma - X\beta)^T W(\sigma - X\beta) \tag{6}$$

where $W = diag(K_{h_m, h_\tau}(M_j - m_0, \tau_j - \tau_0))$ for a Gaussian kernel K with bandwidths h_m and h_τ. σ is the $n \times 1$ vector of oberved implied volatilities, β is the parameter vector. Design matrix X has an intercept.

$$X = \begin{pmatrix} 1 & (M_1 - m_0) & (M_1 - m_0)^2 & (\tau_1 - \tau_0) & (\tau_1 - \tau_0)^2 & (M_1 - m_0)(\tau_1 - \tau_0) \\ \vdots & \vdots & \vdots & \vdots & \vdots & \vdots \\ 1 & (M_n - m_0) & (M_n - m_0)^2 & (\tau_n - \tau_0) & (\tau_n - \tau_0)^2 & (M_n - m_0)(\tau_n - \tau_0) \end{pmatrix}$$

The resulting WLSE is

$$\hat{\beta} = (X^T W X)^{-1} X^T W \sigma \tag{7}$$

6.3 Example: IV Estimation on 2020-03-06

Consider the 102,056 orderbook snapshots that are available for 2020-03-06. Their summary statistics are displayed in Table 2. Local polynomial estimation of the IV smile and it's according first and second derivative can be performed with a subset. The estimated IV for varying moneyness and a fixed $\tau = 0.0384$, meaning maturity is in fourteen days, is presented in Figure 4. A particularly advantageous property of the proposed local polynomial estimation is the lack of assumptions on investor's preferences. Despite the simplicity, stylized facts like the existence of an IV smile is adequately reflected in the estimates.

Parameter	Spot	Strike	Tau	IV
Mean	9093.3250	11029.6075	0.1709	0.6095
Standard Deviation	33.7434	4430.6479	0.1927	0.1226
Minimum	8999.9500	4000	0	0
First Quartile	9068.2400	9000	0.0192	0.5104
Median	9094.4800	9625	0.0575	59.4000
Third Quartile	9119.0400	11000	0.3068	0.6708
Maximum	9179.0200	36000	0.5562	0.1251

Table 2: Summary Statistics for IV Smile Estimation on 2020-03-06

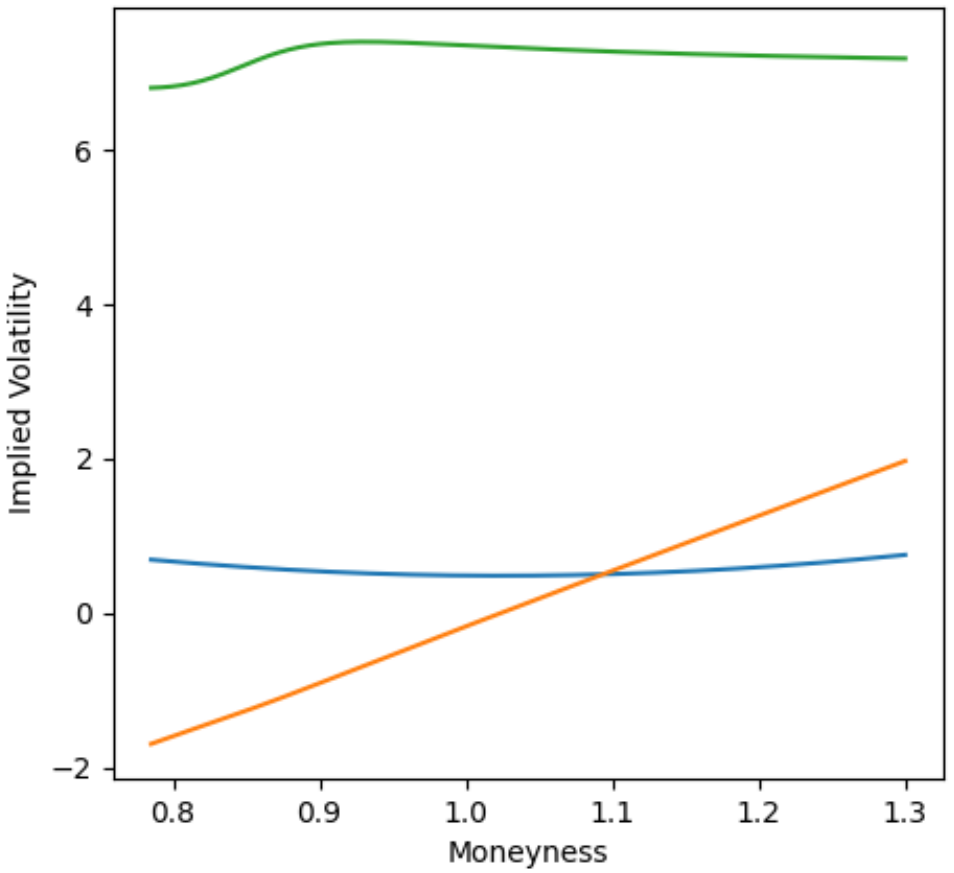

Figure 4: Volatility Smile generated with Local Polynomial Estimation. Observed on 2020-03-06. 14 days until maturity. IV, First Derivative, Second Derivative.

IV Smile

7 SVCJ

The underlying asset process is assumed to be governed by Stochastic Volatility with Correlated Jump (SVCJ) dynamics as introduced by Duffie, Pan, and Singleton (2000). Chen et al. (2018) analyzes the SVCJ framework for Bitcoin and suggests that it surpasses the capabilities of Stochastic Volatility (SV) and Stochastic Volatility with Jumps (SVJ).

7.1 Risk-neutral Measure in Continuous Time

Let $\{S_t\}_{t\in\mathbb{N}}$ denote the Bitcoin price process, $\{d\log S_t\}_{t\in\mathbb{N}}$ it's returns and $\{V_t\}_{t\in\mathbb{N}}$ the volatility process. As in Chen et al. (2018), the SVCJ model is defined as

$$\begin{aligned} d\log S_t &= \mu dt\sqrt{V_t}dW_t^{(S)} + Z_t^y dN_t \\ dV_t = \kappa(\theta - V_t)dt + \sigma_V\sqrt{(V_t)}dW_t^{(V)} &+ Z_t^v dN_t \\ Cov(dW_t^{(S)}, dW_t^{(V)}) &= \rho dt \\ P(dN_t = 1) &= \lambda dt \end{aligned} \tag{8}$$

where κ and θ represent the mean reversion rate and level, $W_t^{(S)}$ and $W_t^{(V)}$ denote standard Wiener processes with correlation ρ. N_t is a Poisson jump process with size Z_t^y and Z_t^v and mean jump arrival rate λ.

The jump sizes are defined as

$$\begin{aligned} Z_t^v &\sim \exp(\mu_v) \\ Z_t \mid Z_t^v &\sim N(\mu_y + \rho_j Z_t^v, \sigma_y^2) \end{aligned} \tag{9}$$

The model is calibrated using a Metropolis-Hastings algorithm as in Perez (2018b). Estimated parameters are reported below.

	Mean	Standard Deviation
α	0.0170	0.0040
β	-0.0570	0.0120
λ	0.0150	0.0060
μ	0.0350	0.0140
μ_v	1.4790	0.3860
μ_y	-0.0020	0.0430
ρ	0.0010	0.0340
ρ_j	-0.0000	0.0200
σ_v	0.0230	0.0050
σ_y	0.4100	0.0540

Table 3: SVCJ Parameters

Chen et al. (2018) regard SVCJ to be particularly useful for Bitcoin price processes. It can be interpreted as an extension of Stochastic Volatility (SV) and Stochastic Volatility Jump (SVJ) models. Additionally, the model structure allows to identify stylized facts of assets, such as the leverage effect between returns and volatility (Ait-Sahalia, Fan, and Li 2011). As many Bitcoin exchanges offer high leverage possibilities, among which Deribit enables Futures trading with a lever of 100, it would be of interest to know if a negative relation between returns and volatility exists. Following Ait-Sahalia, Fan, and Li (2011), the typical reasoning behind such effects is that negative returns increase trader's debt-to-equity ratio, which then causes higher volatility as traders have to adjust their portfolio. Within the SVCJ framework, a leverage effect may be captured in the form of the correlation parameter ρ between the Wiener processes W_t^S and W_t^V.

While the majority of parameters are within the credible intervals estimated by Chen et al. (2018), some parameters differ. First, no significant leverage effect can be found ($\rho = 0.407$ before). Observed BTC/USD prices from 2019-01-01 to 2020-03-01 are used to fit the model. The estimated volatility σ_y is far smaller than the previously reported 2.155 with a credible interval (CI) of [1.142, 3.168]. However, the estimate for volatility of volatility σ_v has tripled from 0.008 (CI [0.007,

0.010]) to 0.0230.

7.2 Physical Measure in Discrete Time

Belaygorod (2005) analyzes the relationship between the risk-neutral and physical measure for different variations of stochastic volatility models, among which SVCJ can be found. While the risk-neutral measure Q is a martingale, the physical measure P is not one due to the existence of risk premia. In consequence, the martingale condition $\mathrm{E}\left(X_{t+1}|F_t\right) = X_t$ does not hold. However, it is possible for E^Q to yield the price of E^P when the latter is discounted at the risk-free rate (Belaygorod 2005). The transformation is based on the change of measure as laid out by Girsanov (1960) and the results are summarized below.

Following Belaygorod (2005) an Euler-Maruyama scheme is employed as a discretization scheme in order to infer the PD.

$$\begin{aligned} \frac{Y_{t\Delta} - Y_{(t-1)\Delta}}{Y_{(t-1)\Delta}} &= \left(\mu_{(t-1)\Delta} - \lambda_{t\Delta}\mathrm{E}_{t\Delta}\left(\Gamma^y_{t\Delta}\right)\right)\Delta + \sqrt{V_{(t-1)\Delta}\Delta\varepsilon^y_{t\Delta}} + \Gamma^y_{t\Delta}J^y_{t\Delta} \\ V_{t\Delta} - V_{(t-1)\Delta} &= \kappa_v(\theta - V_{(t-1)\Delta})\Delta + \sqrt{V_{(t-1)\Delta}\Delta\varepsilon^v_{t\Delta}} + \Gamma^v_{t\Delta}J^v_{t\Delta} \end{aligned} \tag{10}$$

$$\left(\varepsilon^y_{t\Delta}, \varepsilon^v_{t\Delta}\right)^\top \sim \mathrm{N}(0, \Sigma) \tag{11}$$

$$\Sigma = \begin{pmatrix} 1 & \rho\sigma_v \\ \rho\sigma_v & \sigma_v^2 \end{pmatrix} \tag{12}$$

In the discretization scheme, arriving jumps are not Poisson-distributed but Bernoulli random variables with probability λ. A disadvantage of this representation is that there is a non-zero chance for negative volatility due to the behavior of $\varepsilon^v_{t\Delta}$. Such

an effect can be counteracted by using a small Δ (Belaygorod 2005).

7.3 Example: SVCJ Simulation

A Monte Carlo simulation is conducted following Matic (2020). After sampling 100,000 potential asset paths for each SPD on each day, a kernel density estimator $\widehat{p_t}$ is employed in order to extract the PD from the series of returns (Aït-Sahalia, Wang, and Yared 2001). For u sample return paths enumerated from $1, \cdots, M$, the physical density g can be recovered as

$$\widehat{p_t}(u) = \frac{1}{Mh_{MC}} \sum_{i=1}^{M} \frac{K(u_i - u)}{h_{MC}} \tag{13}$$

$$\begin{aligned} P(S_T \leq S) = P(S_t e^u \leq S) = P(u \leq \log(\frac{S}{S_t})) = \int_{-\infty}^{\log(\frac{S}{S_t})} p_t(u) du \\ g_t(S) = \frac{\partial}{\partial S} P(S_t \leq S) = \frac{p_t \log(S/S_t)}{S} \end{aligned} \tag{14}$$

Bandwidth h_{MC} is selected according to Huynh, Kervella, and Zheng (2002b).

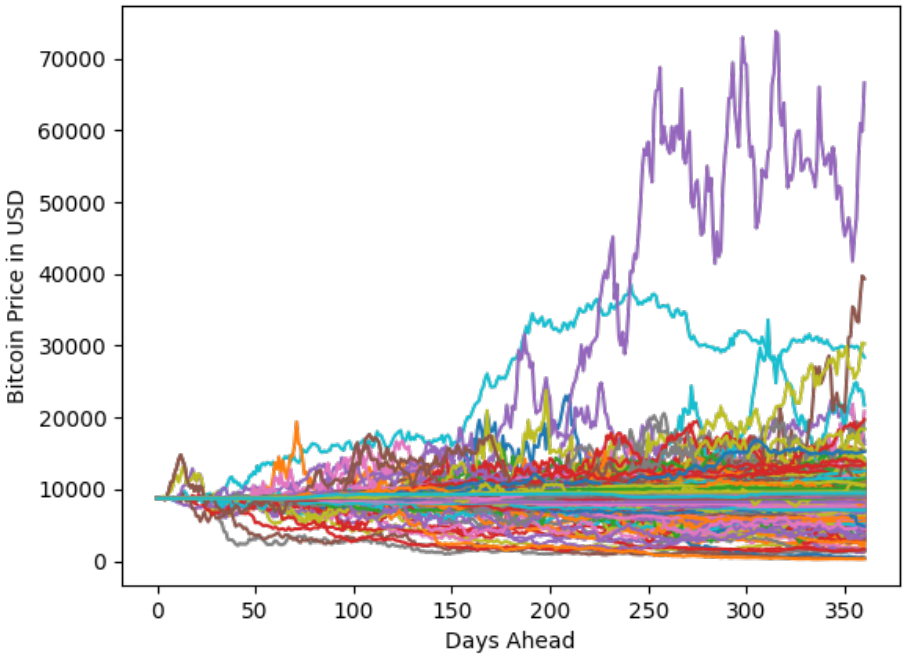

Figure 5: SVCJ Price Simulation from 2020-03-01 for the next 365 Days. 100,000 Paths were sampled. A subset of 1000 Paths is depicted. Parameters were fitted using a Metropolis-Hastings algorithm.

SVCJ

8 Shape Invariant Models

Naturally, having observed Bitcoin options with varying time-to-maturity τ on different points in time, the question of dimension reduction occurs. Shape Invariant Models (SIM) are an approach to collapse different PKs, which share a common time-to-maturity, into a single population curve.

As stated in the Literature Review, Grith, Härdle, and Park (2009) infer empirical, shape invariant PKs for European style DAX options. Based upon the Arrow-Pratt measure of absolute risk aversion (ARA), they argue that the link between the market's risk neutral pricing to subjective, investor-specific risk adaptive behavior, is the pricing kernel.

8.1 Algorithm

Following Grith, Härdle, and Park (2009), let $\{Y_{tj}, t = 1, \cdots, T; j = 1, \cdots, n\}$ be a sample of curves measured at u_j in a real-valued interval J.

$$Y_{tj} = K_t(u_j) + \varepsilon_{tj} \tag{15}$$

where the errors ε_{tj} are independent and identically distributed with a zero mean and a constant variance.

Consider the set of curves $\{Y_{tj}\}$ to be a set of PKs measured at a different point in time, but with a common time-to-maturity τ. Then each PK can be regarded as a shift from a reference kernel K_0 under

$$K_t(u) = \theta_{t1} K_0(\frac{u - \theta_{t3}}{\theta_{t2}}) + \theta_{t4} \tag{16}$$

The parameters θ_{tj} can be estimated using the algorithm specified in Grith, Härdle, and Park (2009), which is presented in the following.

Initialization:

- Estimate individual regression functions K_t using a nonparametric smoother (e.g. Nadaraya Watson Estimator)
- Set starting values for θ_{tk} for each point in time
- Initial estimate of the reference curve $K_0^{(0)}(u) = T^{-1} \sum_{t=1}^{T} \widehat{K}_t(\theta_{t2}^{(0)} u + \theta_{t3}^{(0)})$

In every iteration, for each θ_j, update and normalize the parameters and eventually the reference kernel until convergence is reached.

Minimize the objective function

$$\arg\min_{\theta_{tj}} \int_{\mathbb{R}} \{\widehat{K}_t(\theta_{t2}^{(0)} u + \theta_{t3}^{(0)}) - \theta_{t1} K_0^{r-1}(u) - \theta_{t4}\}^2 w(u) du \tag{17}$$

Normalize Parameters

$$\begin{aligned} \theta_{tj}^r &\leftarrow \frac{\theta_{tj}^r}{\sum_t \theta_{tj}^r} \qquad \text{for} \quad j = (1,2) \\ \theta_{tj}^r &\leftarrow \theta_{tj}^r - T^{-1} \sum_{t=1}^{T} \theta_{tj}^r \qquad \text{for} \quad j = (3,4) \end{aligned} \tag{18}$$

Update Reference Kernel

$$K_0^{(r)}(u) = T^{-1} \sum_{t=1}^{T} \widehat{K}_t(\theta_{t2}^{(r)} u + \theta_{t3}^{(r)}) \tag{19}$$

The weight function $w(u)$ ensures that functions are compared in a domain where the common features are defined. The presented algorithm converges even for a larger number of pricing kernels in a reasonable time.

8.2 Estimated Shape Invariant Pricing Kernels

Standard literature suggests the shape of PKs to be decreasing (increasing) for higher (lower) wealth levels, which suggests risk-averse investor preferences (Grith, Härdle, and Park 2009). The empirically estimated Bitcoin PKs support these results. Most PKs are decreasing when wealth increases. When time-to-maturity approaches zero, PKs have a Gaussian shape.

Moneyness m is defined as the ratio of spot to strike price. Usually, a SPD is depicted as a density over a range of strike prices. In order to ensure comparability of the PKs, moneyness is chosen as the domain. Since the end-of-day spot price is used to calculate moneyness, an increase in moneyness is actually associated with a decrease in wealth. Vice versa, a decrease in moneyness is associated with an increase in wealth.

The empirical PKs typically share the similarity of becoming large in the right tail. This observation indicates a tremendous level of risk averseness among some market participants. Apparently a substantial share of investors are consistently insuring themselves against exceptionally high, negative returns and demonstrate the willingness to pay substantial risk premia.

In the following, a selection of estimated shape invariant pricing kernels is presented for instruments which have a common time to maturity, as indicated by the subsection names. The respective observation date of each pricing kernel, which is calculated for each instrument, is depicted in the legend. Reported Thetas are the horizontal and vertical shift parameters as in Equation (16). Their purpose is to link the reference kernel to a fixed, empirical pricing kernel.

8.2.1 Maturity in 9 Days

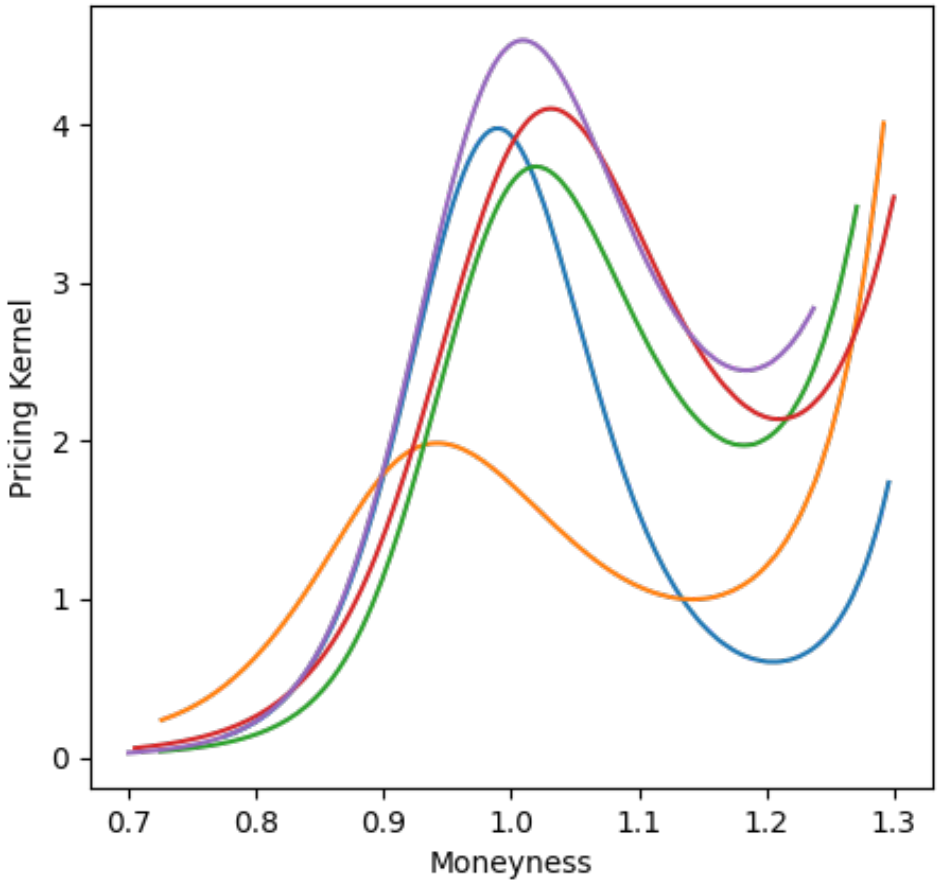

Figure 6: Pricing Kernels estimated on different observation dates. Despite a six month time window, the shape is similar. Maturities of the individual PKs: 2020-03-13, 2020-04-10, 2020-06-26, 2020-06-05, 2020-09-18.

SIM

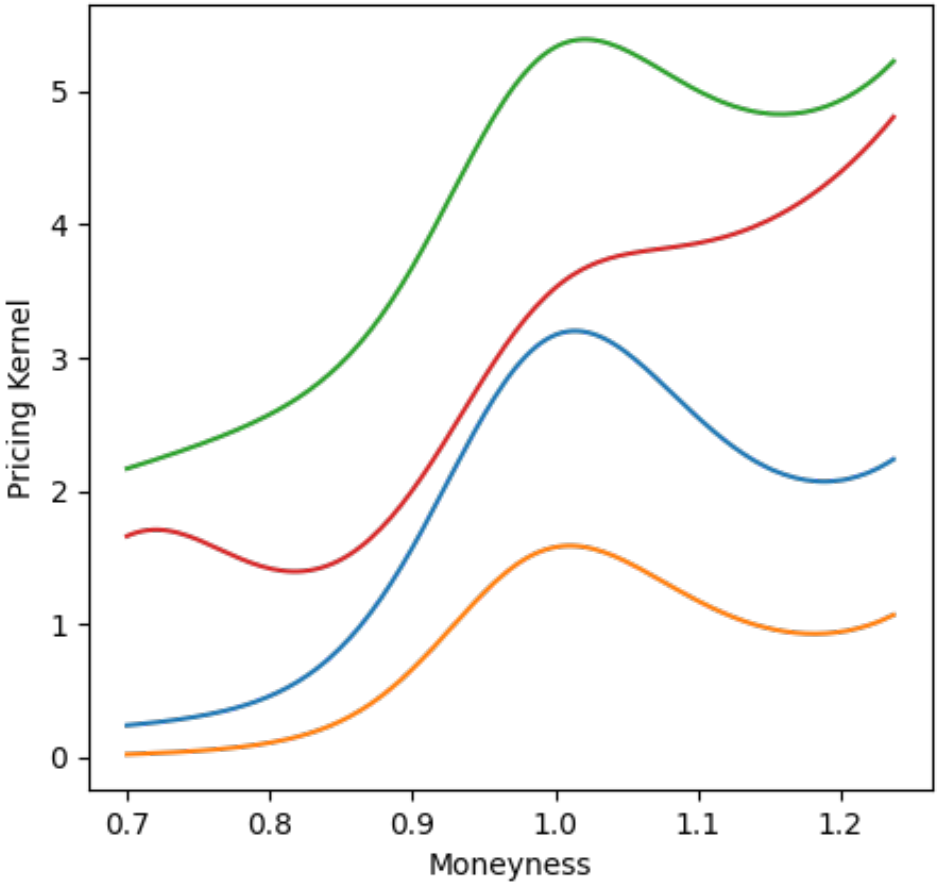

Figure 7: Convergence of the Shape Invariant Pricing Kernel. Final Iteration.

SIM

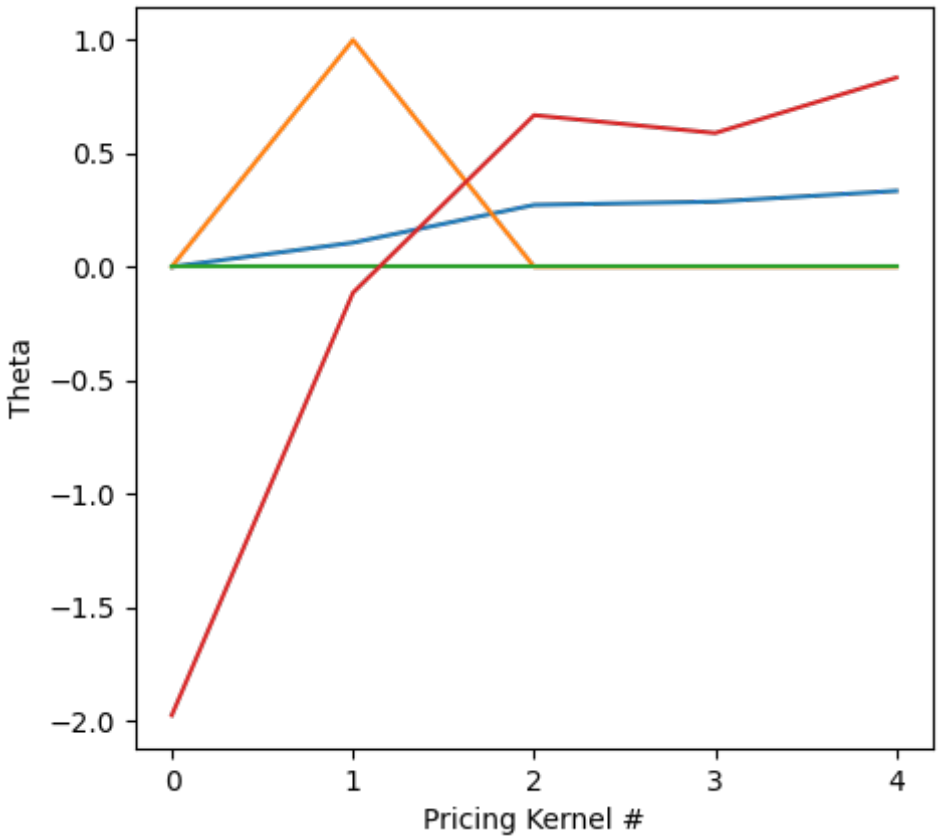

Figure 8: Estimated parameters for horizontal and vertical shift. Theta 1, Theta 2, Theta 3, Theta 4.

QSIM

8.2.2 Maturity in 18 Days

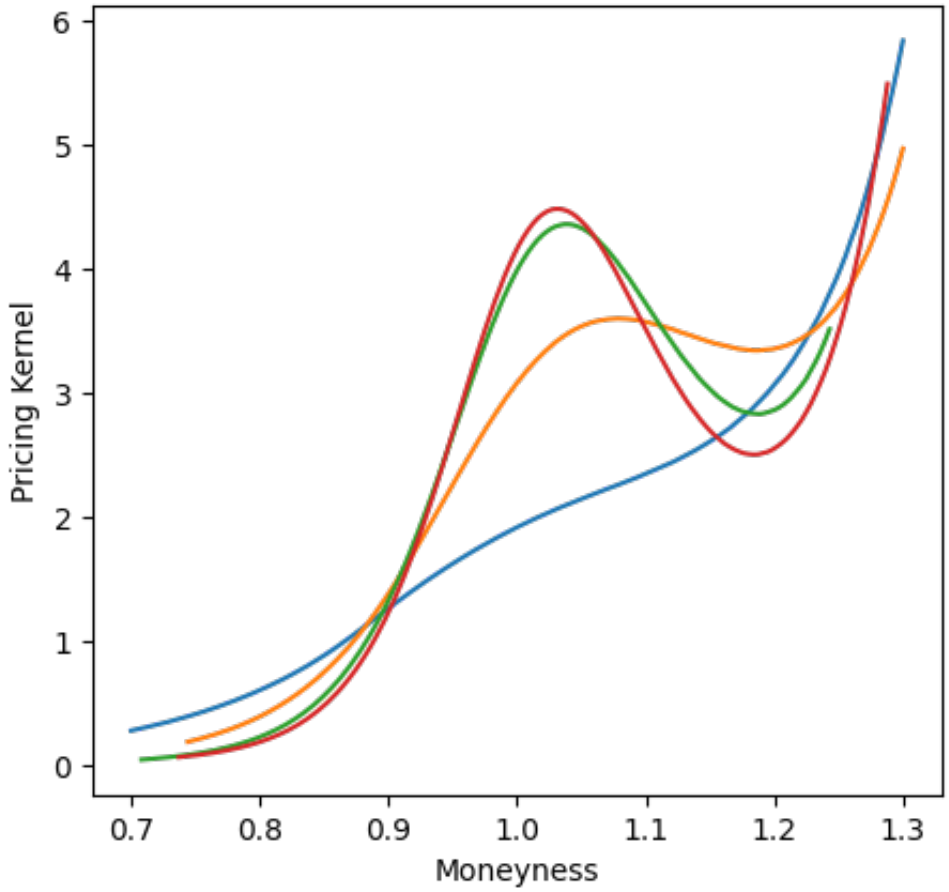

Figure 9: Pricing Kernels estimated on different observation Dates. Maturities of the individual PKs: 2020-04-24, 2020-06-26, 2020-07-31, 2020-10-09.

QSIM

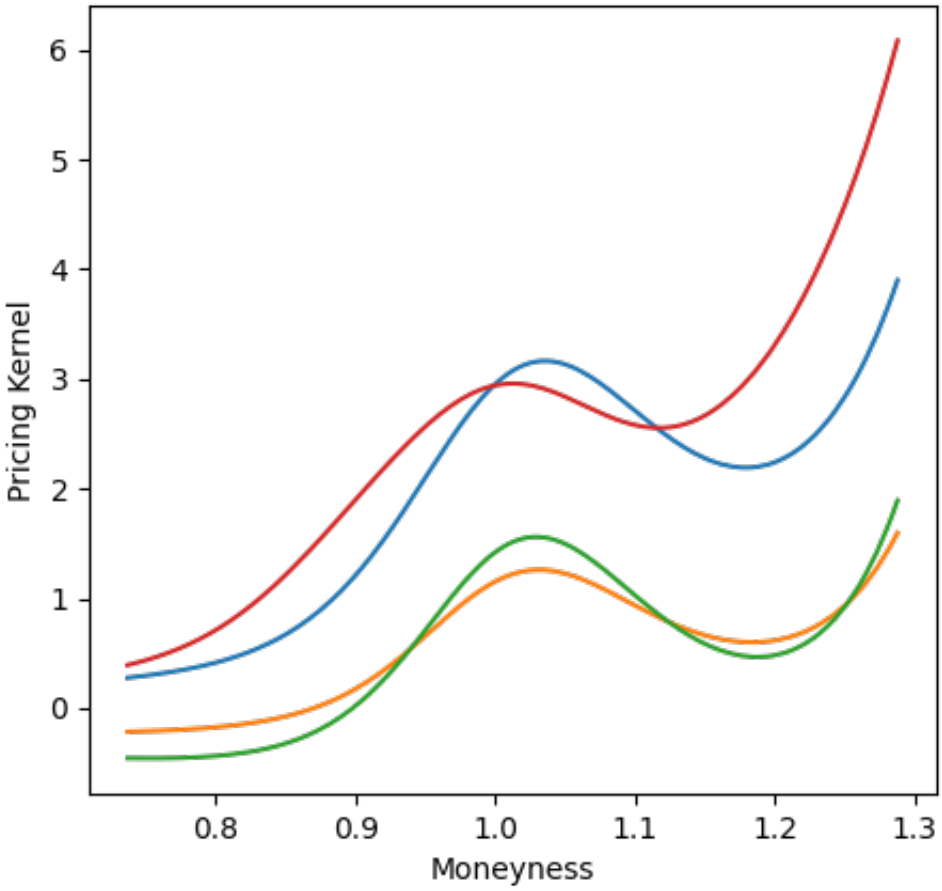

Figure 10: Convergence of the Shape Invariant Pricing Kernel. Final Iteration.

SIM

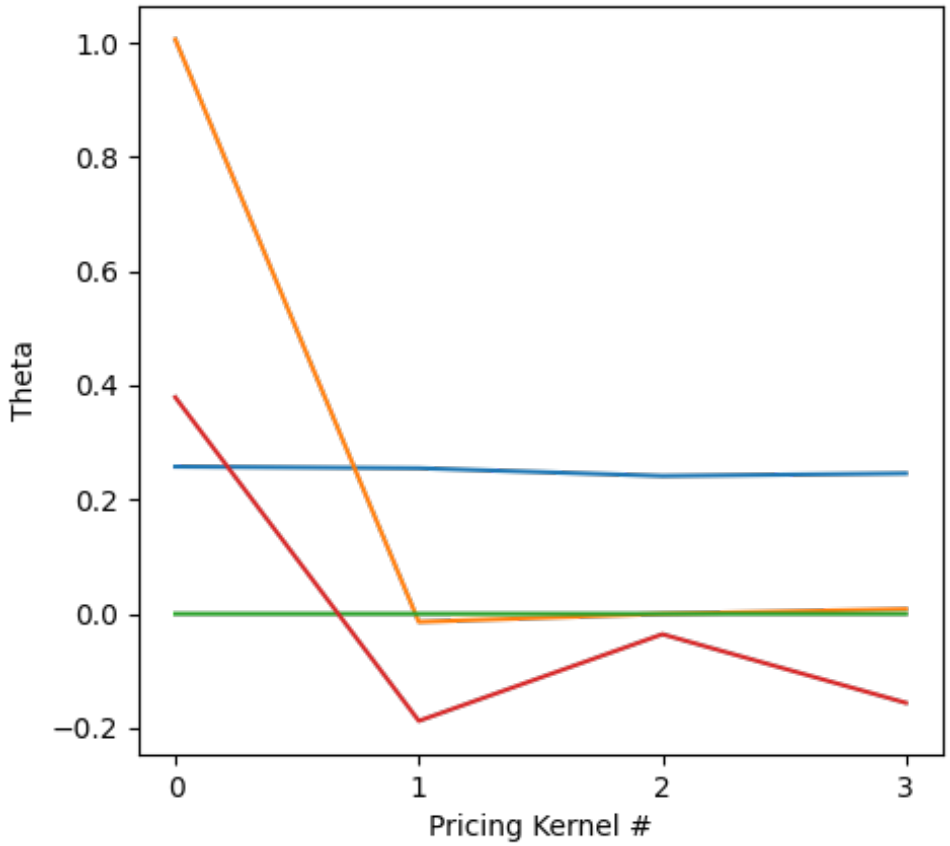

Figure 11: Estimated Parameters for horizontal and vertical shift.Theta 1, Theta 2, Theta 3, Theta 4.

QSIM

9 Trading on Density Deviations

Knowledge of the SPD unveils investor preferences for all possible Bitcoin price realizations at a pre-specified point in time. The SPD has a forward-looking nature since it contains information about investor preferences and their expectations about the future. Acknowledging that investors may misjudge, over- or underemphasize certain outcomes, the argument can be made that a simulation from a neutral point of view may yield better results. If this holds true, then a profitable trading strategy might be found that may counteract shortcomings of investor valuations.

The estimated PKs indicate that investors are willing to insure themselves against large, negative returns. This willingness is measurable by the substantial premia for FOTM puts that are being offered and traded. Since SPDs and PDs are probability densities, they are formally required to be strictly positive and integrate to one. This is verified for all estimated densities. If investor's are willing to insure themselves against large, negative returns, then this implies additional probability mass on one end of the tail, which means a comparative lack of probability mass somewhere else on the domain. To continue with the example, if investors put too much weight on left-sided fat tail events, their behavior may be counteracted by shorting FOTM puts and buying ATM puts (and vice versa for calls). As a result, a simple trading strategy may be constructed, consisting of a call spread and a put spread. Two spreads are traded on the evening of each day when the SPD and the PD have been calculated for that day and a fixed time-to-maturity τ. Both are held until maturity and standard Deribit transaction costs are applied.

On the left-hand side of Figure 12 the SPD is compared to the PD. The right-hand side shows which instrument can be traded for each region, depending on where the deviation between the densities is large. If multiple instruments are available, then the one that is closest ATM is preferred. The strategy can be simulated if a

call spread and a put spread can be traded, hence if at one instruments exist in each of the designated four regions on the moneyness domain.

Recall that moneyness m is defined as the ratio of spot to strike price. Usually, a SPD is depicted as a density over a range of strike prices. In order to ensure comparability of the PKs, moneyness is chosen as the domain. Since the end-of-day spot price is used to calculate moneyness, an increase in moneyness is actually associated with a decrease in wealth (negative return). Vice versa, a decrease in moneyness is associated with an increase in wealth (positive return).

For example the densities observed on 2020-03-18, depicted on Figure 14, reveil that investors are willing to pay a substantial premium for puts, as the difference in the right tail shows. Naturally the payoff of the trades committed on each day varies due to degree of density deviations as well as available instruments and direction (long/short). One example of a payoff function is depicted on Figure 13 for the densities observed on 2020-05-18, where time-to-maturity is four days.

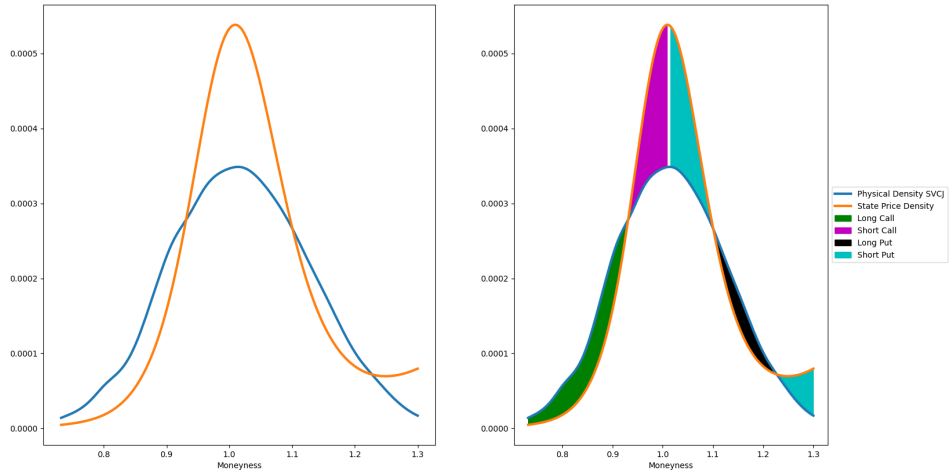

Figure 12: State Price Density vs. Physical Density on 2020-05-18 for 4 Days until Maturity.

Strategies

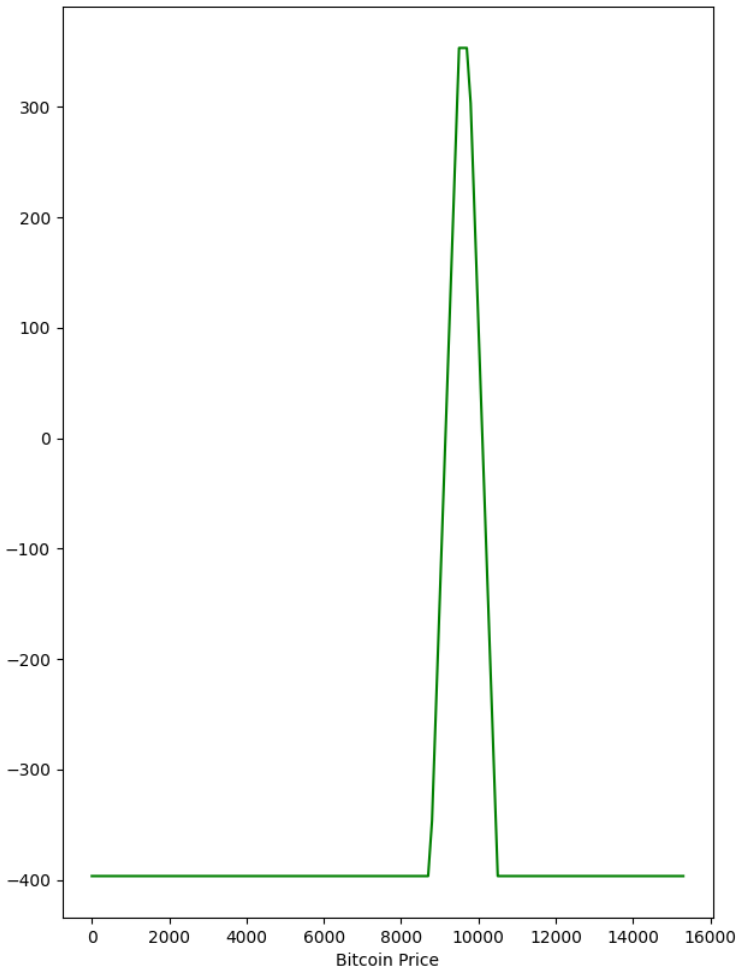

Figure 13: Payoff Function for the Trading Strategy on 2020-05-18 for 4 Days until Maturity. Denoted in USD.

Strategies

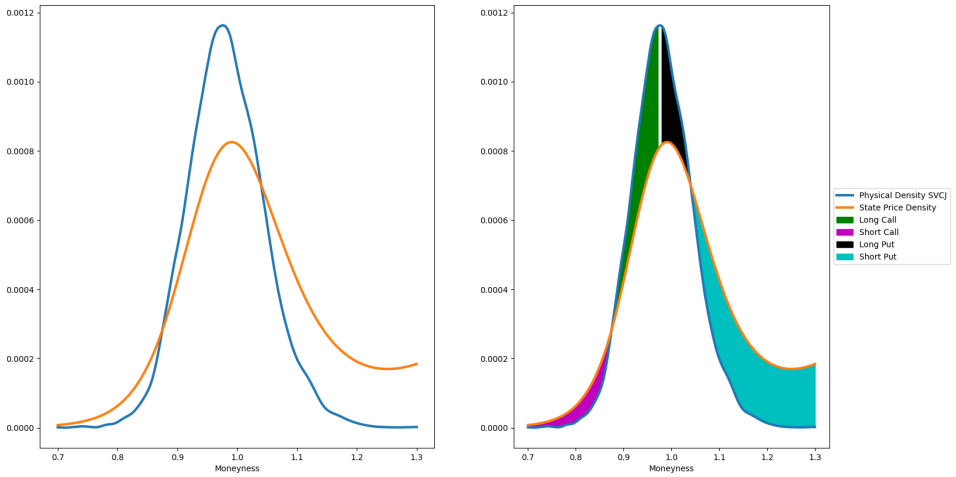

Figure 14: State Price Density vs. Physical Density on 2020-03-18 for 2 Days until Maturity.

Strategies

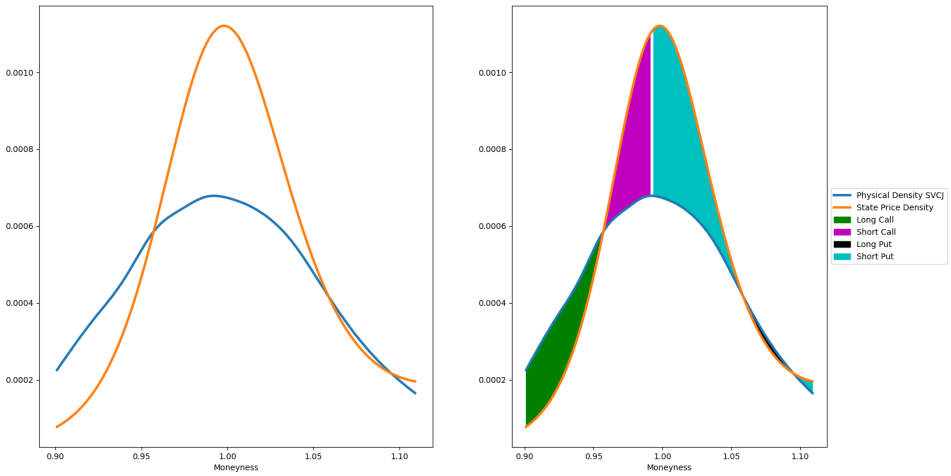

Figure 15: State Price Density vs. Physical Density on 2020-05-25 for 2 Days until Maturity.

Strategies

Across all observations and from the beginning of March until mid December, a set of SPDs, PDs and eventually PKs has been created. For each PK, the discussed strategy is employed. A total of 53 trading opportunities have been identified and simulated. The rather small amount of trading simulations indicates that the SPD and PD do not allow for too large deviations, which leads to the conclusion that market inefficiencies can rarely be found using these methods.

The Profit and Loss distribution (PnL) is estimated by means of a Gaussian kernel density estimator applied to the absolute profits (Virtanen et al. 2020). Deribit (2020d) charges a fee of 0.015% on the delivery of options. As all options in the simulated strategy are held until maturity, the fee is subtracted at maturity. As the PnL distribution shows, the expected value is positive, but comes at the price of a large variance. The Sharpe Ratio, which summarizes the performance of an investment strategy over the risk free rate, is 0.1598. The risk-free rate is set to zero.

Despite the large amount of orderbook observations, few trading opportunities could actually be identified. In conjunction with the low Sharpe Ratio we can conclude that the market is relatively efficient since the SPD and the PD are often too close to create a valid trading strategy in the defined manner. Those opportunities that are identifiable, create a positive payoff at such a high cost (standard deviation) that more profitable and less risky strategies should exist.

While the proposed trading strategy performs relatively well, the risk is too high to actually be preferable over other trading strategies. Nevertheless, a variety of modifications can be implemented in order to counter the shortcomings. Comparing the results with Huynh, Kervella, and Zheng (2002a), a common property of distribution based trading strategies appears to be heavy directional risk. Delta-Hedging may offset the directional risk which increases the strategy's variance to

such an extend that it is very likely to find less risky strategies, which come at a similar payoff.

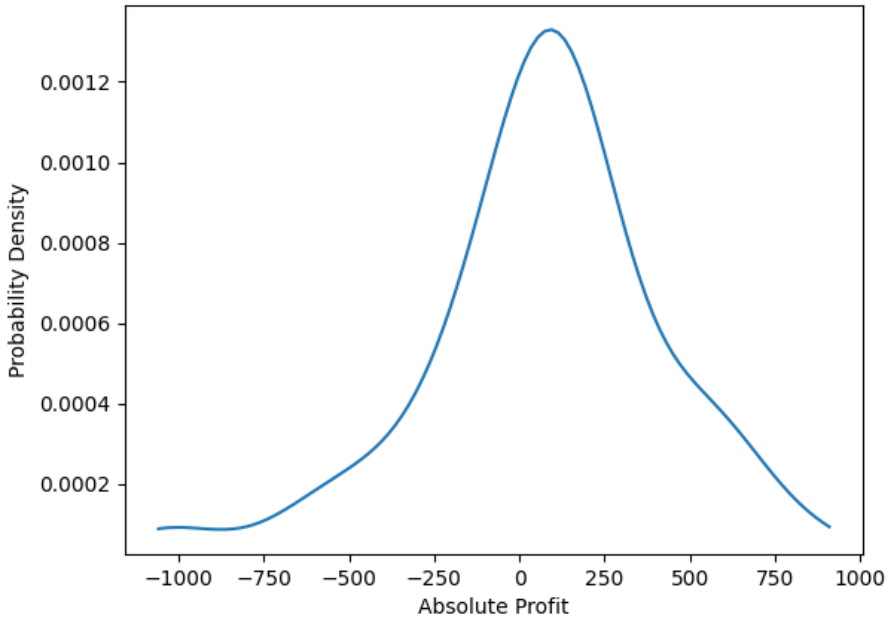

Figure 16: Profit and Loss Distribution of the Trading Simulation. Denoted in USD.

PnL

10 Conclusion

A novel data set containing high-frequency orderbook snapshots of the major Bitcoin Derivatives exchange Deribit has been analyzed in this thesis. The market is found to price contracts reasonably in terms of implied volatility. State Price Densities are estimated for various instruments in order to allow arbitrage-free pricing for arbitrary options and the provided Quantlets allow practicioners to use the provided results. A Stochastic Volatility with Correlated Jumps framework is fitted and found to adequately describe the Bitcoin asset process. Pricing kernels are calculated and evaluated. Those, which share a common time-to-maturity also share a common shape, which is summarized in the Shape Invariant Pricing Kernel. This allows to study the evolution of pricing kernels over time as well as their common features. It also provides a link to study investor's absolute risk aversion. A trading strategy has been designed based on deviations between the physical density and the State Price Density. As the low Sharpe Ratio indicates, the expected profit does not outweigh the risk.

11 References

Ait-Sahalia, Yacine, Jianqing Fan, and Yingying Li. 2011. "The Leverage Effect Puzzle: Disentangling Sources of Bias at High Frequency." Working Paper 17592. Working Paper Series. National Bureau of Economic Research. https://doi.org/10.3386/w17592.

Aït-Sahalia, Yacine, Yubo Wang, and Francis Yared. 2001. "Do Option Markets Correctly Price the Probabilities of Movement of the Underlying Asset?" *Journal of Econometrics* 102 (1): 67–110. https://doi.org/https://doi.org/10.1016/S0304-4076(00)00091-9.

Aït-Sahalia, Yacine, and Andrew W. Lo. 1998. "Nonparametric Estimation of State-Price Densities Implicit in Financial Asset Prices." *The Journal of Finance* 53 (2): 499–547. https://doi.org/https://doi.org/10.1111/0022-1082.215228.

Belaygorod, Anatoliy. 2005. "Solving Continuous Time Affine Jump-Diffusion Models for Econometric Inference."

Breeden, Douglas T., and Robert H. Litzenberger. 1978. "Prices of State-Contingent Claims Implicit in Option Prices." *The Journal of Business* 51 (4): 621–51. http://www.jstor.org/stable/2352653.

Chen, Cathy, Wolfgang Karl Härdle, Ai Hou, and Weining Wang. 2018. "Pricing Cryptocurrency Options: The Case of Crix and Bitcoin." *SSRN Electronic Journal*, January. https://doi.org/10.2139/ssrn.3159130.

Coinmarketcap. 2021. "Coinmarketcap - Trading Volume." 2021. https://coinmarketcap.com/exchanges/deribit/.

Cox, J. C., J. Ingersoll, and S. A. Ross. 1985. "A Theory of the Term Structure of Interest Rates", Econometrica 53, 385-407." In.

Deribit. 2020a. “Deribit Btc-Usd Index.” 2020. https://www.deribit.com/main#/indexes.

———. 2020b. “Deribit Insurance Fund.” 2020. https://www.deribit.com/main#/insurance.

———. 2020c. “Deribit Market Maker Obligations.” 2020. https://www.deribit.com/pages/docs/options.

———. 2020d. “Deribit Market Maker Obligations.” 2020. https://www.deribit.com/pages/information/fees.

Duffie, Darrell, Jun Pan, and Kenneth Singleton. 2000. “Transform Analysis and Asset Pricing for Affine Jump-Diffusions.” *Econometrica*, 1343–76.

Girsanov, I. V. 1960. “On Transforming a Certain Class of Stochastic Processes by Absolutely Continuous Substitution of Measures.” *Theory of Probability & Its Applications, 5, 285-301.*

Grith, Maria, Wolfang Härdle, and Juhyun Park. 2009. “Shape Invariant Modelling Pricing Kernels and Risk Aversion.”

Heston, Steven L. 1993. “A Closed-Form Solution for Options with Stochastic Volatility with Applications to Bond and Currency Options.” *The Review of Financial Studies* 6 (2): 327–43. http://www.jstor.org/stable/2962057.

Huynh, Kim, Pierre Kervella, and Jun Zheng. 2002a. “Estimating State-Price Densities with Nonparametric Regression.” SFB 373 Discussion Papers 2002,40. Humboldt University of Berlin, Interdisciplinary Research Project 373: Quantification; Simulation of Economic Processes. https://EconPapers.repec.org/RePEc:zbw:sfb373:200240.

———. 2002b. “Estimating State-Price Densities with Nonparametric Regression,”

January. https://doi.org/10.1007/978-3-662-05021-7_8.

Matic, Jovanka. 2020. “Hedging Strategies Under Jump-Induced Market Incompleteness.” Master’s thesis, Humboldt-Universität zu Berlin, Wirtschaftswissenschaftliche Fakultät. https://doi.org/http://dx.doi.org/10.18452/21310.

Nakamoto, Satoshi. 2009. “Bitcoin: A Peer-to-Peer Electronic Cash System.” http://www.bitcoin.org/bitcoin.pdf.

Pascucci, Andrea, and R Agliardi. 2011. “PDE and Martingale Methods in Option Pricing.” In, 429–95.

Perez, Ivan. 2018a. “Graphical User Interface for Pricing Cryptocurrency Options Under the Stochastic Volatility with Correlated Jumps Model.” Master’s thesis, Humboldt-Universität zu Berlin, Wirtschaftswissenschaftliche Fakultät. https://doi.org/http://dx.doi.org/10.18452/19509.

———. 2018b. “Graphical User Interface for Pricing Cryptocurrency Options Under the Stochastic Volatility with Correlated Jumps Model.” Master’s thesis, Humboldt-Universität zu Berlin, Wirtschaftswissenschaftliche Fakultät. https://doi.org/http://dx.doi.org/10.18452/19509.

Quandl. 2020. “WIKI Quandl End-of-Day Data.” 2020. https://www.quandl.com/data/.

Rookley, Cameron. 1997. “Fully Exploiting the Information Content of Intra Day Option Quotes: Applications in Option Pricing and Risk Management.”

Virtanen, Pauli, Ralf Gommers, Travis E. Oliphant, Matt Haberland, Tyler Reddy, David Cournapeau, Evgeni Burovski, et al. 2020. “SciPy 1.0: Fundamental Algorithms for Scientific Computing in Python.” *Nature Methods*.

Declaration of Authorship

I, Julian Winkel, hereby confirm that I have written this thesis independently. All sources, that have contributed to this thesis are marked as such. This work has neither been submitted to any examination nor published before.

19.02.2021